Potential for Geologic Records of Coseismic Uplift and Megathrust Rupture along the Nicoya Peninsula, Costa Rica

Authors: Spotila, James A., Marshall, Jeff, DePew, Keith, Prince, Philip S., and Kennedy, Lisa

Source: Journal of Coastal Research, 32(2) : 387-396

Published By: Coastal Education and Research Foundation

URL: https://doi.org/10.2112/JCOASTRES-D-14-00151.1

Journal of Coastal Research	32	2	387–396	Coconut Creek, Florida	March 2016

Potential for Geologic Records of Coseismic Uplift and Megathrust Rupture along the Nicoya Peninsula, Costa Rica

James A. Spotila[†]*, Jeff Marshall[‡], Keith DePew[†], Philip S. Prince[†], and Lisa Kennedy[†]

[†]Department of Geosciences
Virginia Polytechnic Institute and State University
Blacksburg, VA 24061, U.S.A.

[‡]Geological Sciences Department
California State Polytechnic University, Pomona
Pomona, CA 91768, U.S.A.

www.cerf-jcr.org

www.JCRonline.org

ABSTRACT

Spotila, J.A.; Marshall, J.; DePew, K.; Prince, P.S., and Kennedy, L., 2016. Potential for geologic records of coseismic uplift and megathrust rupture along the Nicoya Peninsula, Costa Rica. *Journal of Coastal Research,* 32(2), 387–396. Coconut Creek (Florida), ISSN 0749-0208.

This study presents the first paleoseismic investigation of the Middle America subduction zone at the Nicoya Peninsula, Costa Rica. This megathrust has been intensely studied over the past decade using a range of geologic and geophysical techniques, and it experienced interplate rupture in 2012 (moment magnitude 7.6). Despite many factors that could hinder preservation of a paleoseismic record in this coastal environment, including complex deposition in a tropical mangrove setting, this reconnaissance identifies two sites where stratigraphic evidence may record relative sea-level changes associated with Holocene earthquakes. Although more work is required to better constrain the timing and nature of these events, this study suggests that the Tamarindo and Playa Carrillo estuaries contain possible paleoseismic records. At the main study site of Tamarindo, alternations between mud and peat below 1 m in depth may record relative sea-level change associated with multiple earthquakes between ~5 and 8 ka. However, this site offers no paleoseismic evidence of late-Holocene earthquakes. Much younger stratigraphy occurs at a Playa Carrillo, where mud-peat alternations from 200 to 500 years ago could represent recent coseismic ground motions. The work presented here is limited to litho- and chronostratigraphy, however, and full interpretation of the relative sea-level histories of both sites will require quantitative, high-resolution biostratigraphic analysis. Although the results suggest paleoseismic records exist along the Nicoya Peninsula, they appear fragmentary and complex and ultimately may not provide a continuous, high-resolution paleoseismic record like those obtained at other subduction zones worldwide.

ADDITIONAL INDEX WORDS: *Subduction zone earthquakes, estuary, mangrove, relative sea-level change, coastal uplift.*

INTRODUCTION

Megathrust seismogenesis is dynamically controlled as a complex system involving numerous interconnected components, including plate roughness, deformation, mantle convection, hydrology, heat flow, sediment cycling, metamorphism, and other processes (DeShon *et al.*, 2006; Hyndman and Wang, 1993; Kinoshita *et al.*, 2006). Despite obvious societal relevance, it remains incompletely understood how physical and chemical processes affect mechanical behavior, which subduction zones are capable of great earthquakes, and the scale of inherent variability in mode of megathrust rupture (Bilek, Schwartz, and DeShon, 2003; Cisternas *et al.*, 2005; McCaffrey, 2008; Satake and Atwater, 2007; Schwartz, 1999; Sieh *et al.*, 2008; Stein and Okal, 2007).

Extensive effort has been invested in understanding the seismogenesis of the Middle America subduction zone at the Nicoya Peninsula, Costa Rica (see MARGINS Staff, 2004). The behavior of this megathrust at timescales exceeding the instrumental record, however, is poorly known. Paleoseismology is generally the only methodology able to connect a real-time, dynamic, physical-chemical understanding of a fault with its seismogenic behavior over numerous seismic cycles. Perturbations to sedimentary deposits and other features can record the occurrence of large earthquakes as shaking events, tsunamis, and changes in elevation relative to sea level (Carver and McCalpin, 1996). Geologic evidence has contributed significantly to understanding the behavior and hazards of subduction zones with moderate (>0.3 ka) recurrence intervals and significant (>1 m) relative sea-level change in temperate coastal environments, particularly from environments that exhibit strong contrast between freshwater and saline intertidal deposits (*e.g.* Atwater, 1987; Cisternas *et al.*, 2005; Nelson, Shennan, and Long, 1996; Sawai *et al.*, 2004; Shennan *et al.*, 2014). This approach is more challenging in the complex deposits of tropical mangrove-dominated wetlands, yet it has locally been shown to be effective at documenting paleoseismic events and relative sea-level change (Belperio, Harvey, and Bourman, 2002; Berkeley *et al.*, 2009; Dura *et al.*, 2011; Grand Pre *et al.*, 2012; Jankaew *et al.*, 2008; Monecke *et al.*, 2008; Rashid *et al.*, 2013). The use of recent coastal stratigraphy to document paleoearthquakes may be even more challenging where recurrence intervals are short (<0.1 ka) or coseismic motions are small (<1 m). These and other factors make the feasibility of obtaining a paleoseismic record from the Middle America Trench uncertain. We have explored this feasibility by reconnaissance examination of estuarine deposits along the Nicoya Peninsula.

The Nicoya Peninsula in northern Costa Rica is underlain by an emergent forearc of the Middle America Trench, where the

DOI: 10.2112/JCOASTRES-D-14-00151.1 received 5 August 2014; accepted in revision 10 April 2015; corrected proofs received 18 June 2015; published pre-print online 3 August 2015.
*Corresponding author: spotila@vt.edu

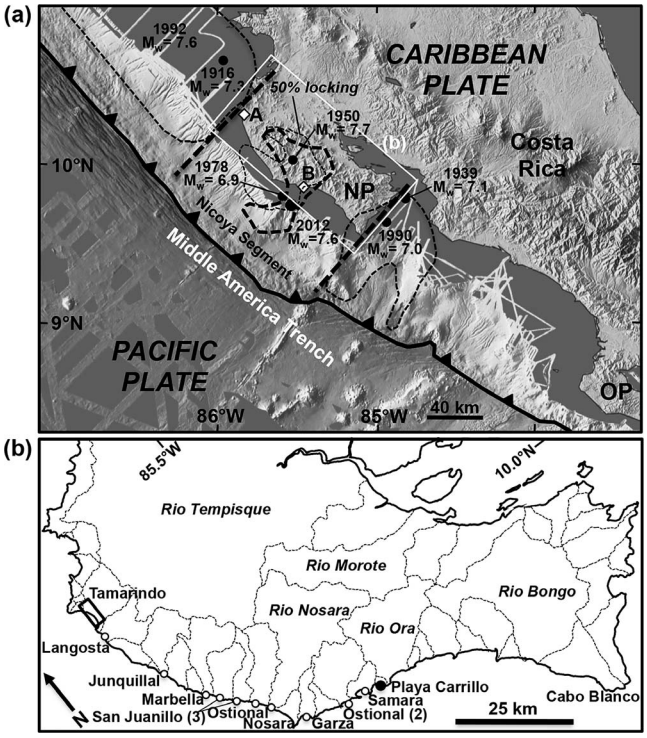

Figure 1. (a) Location of the Nicoya Peninsula (NP) along the Middle America Trench. Distribution of major historical interplate earthquakes are shown, including epicenters for major recent events and rupture areas for 2012 (coseismic slip >1.2 m; Yue *et al*., 2013), 1992, and 1990 (Protti *et al*., 2014). Thin dashed line denotes region of 50% plate interface locking prior to the 2012 earthquake (Feng *et al*., 2012). Heavy dashed lines denote the Nicoya seismic gap. Locations of the two main field sites are marked by A (Tamarindo) and B (Carrillo). White box indicates location of drainage basins seen in Figure 1b. Digital elevation model (National Aeronautics and Space Administration-Shuttle Radar Topography Mission) and offshore bathymetry (Helmholtz Centre for Ocean Research multibeam) are courtesy of C. Ranero. (b) Drainage basins of the Nicoya Peninsula. Dashed lines denote catchment areas of rivers draining the peninsula. Locations of Tamarindo and Carrillo are shown. Open circles are other estuaries or wetlands examined in this study.

~20–25 Ma Cocos plate subducts beneath the Caribbean plate and Panama block at ~8.3 cm/y (DeMets, Gordon, and Argus, 2010) (Figure 1a). A clear Benioff zone defines the limits of a 6°–13° dipping seismogenic megathrust at a depth of ~10–28 km (DeShon *et al*., 2006; Newman *et al*., 2002; Protti, Guendel, and McNally, 1995; Schwartz and DeShon, 2007). Because of the roughness of the subducting slab, the Middle America Trench is segmented and has tended to fail only in moderate interplate events (*i.e*. <M8, length <200 km). Segment boundaries and other factors, such as the presence of fluids, result in significant variation in megathrust behavior, including the distribution of locking and upper-plate deformation (Audet and Schwartz, 2013; DeShon *et al*., 2006; Feng *et al*., 2012; Fisher *et al*., 1998; Iinuma *et al*., 2004; Newman *et al*., 2002; Norabuena *et al*., 2004).

Historic earthquakes demonstrate that the trench is seismogenic beneath the Nicoya Peninsula (Figure 1a). Eight large earthquakes ($M > 7$) have occurred in this area in the past 200 years (Figure 1a) (Protti *et al*., 2014). Four of these occurred to the NW or SE and define the Nicoya segment. The other four (1853, 1900, 1950, 2012) are considered to have been caused by interplate rupture of the Nicoya segment itself (Iinuma *et al*., 2004; Protti, Guendel, and Malavassi, 2001; Protti *et al*., 2014). The recent earthquake of 5 September 2012 (moment magnitude [M_w] = 7.6) ruptured a partially locked zone in the middle of the Nicoya segment, releasing the accumulated strain in the region of the Nicoya seismic gap (Nishenko, 1989; Protti, Guendel, and Malavassi, 2001; Protti *et al*., 2014). This event had a maximum interplate slip of 4.4 m and maximum geodetically determined coastal uplift of 0.53 m and geologically observed uplift of 0.67 m, thus recovering nearly all of the accumulated strain since the penultimate event in 1950 (M_w = 7.7) (Protti *et al*., 2014; Yue *et al*., 2013). The rupture did not extend through the entire up-dip portion of the geodetically defined locked zone (Figure 1a) (Feng *et al*., 2012), however, suggesting the potential for a future M~7 event offshore (Protti *et al*., 2014; Yue *et al*., 2013).

The similarity in size and rupture area of the 2012 and 1950 events suggests that these are representative for interplate earthquakes on the Nicoya segment (Marshall and Anderson, 1995; Protti *et al*., 2014). Because of proximity to the trench (~60 km), the central Nicoya coastline (including our Carrillo site) experiences interseismic subsidence at ~1 cm/y, which is recovered by 0.5–1.0 m coseismic uplift every ~50 years (Iinuma *et al*., 2004; Marshall and Anderson, 1995; Protti *et al*., 2014). The unusually short recurrence interval could give the Nicoya Peninsula unique value for understanding the dynamic processes that control subduction zone seismogenesis. A complicating factor is that the pattern of elastic subsidence and uplift should decrease away from the center of the locked zone to zero at segment boundaries, but it is unclear where our Tamarindo site falls along this gradient of decreasing strain (Figure 1a). Another complication is that superimposed on the seismic cycle is a component of long-term net uplift, which increases steadily from ~0.1 mm/y along the northern Nicoya Peninsula to 1–2 mm/y at Cabo Blanco in the SE (Marshall *et al*., 2012).

METHODS

There are several potential problems for finding reliable paleoseismic sites in the Nicoya Peninsula. The historical high frequency and small magnitude of relative sea-level change could hinder preservation of a useful paleoseismic record, particularly in the complex, heavily bioturbated deposits of a tropical mangrove environment. Given the short recurrence interval, a paleoseismic record would require rapid sedimentation, such that the sedimentary or paleontological environmental indicators would be preserved and stratigraphically separated into recognizable packages. The expected smallness of the coseismic sea-level changes relative to the noise associated with the large tidal range of the Nicoya coast (~2–3 m) may be another potential hindrance to stratigraphic recognition of paleoseismic events. Additionally, the Nicoya coast experiences coseismic uplift, whereas subduction zone paleoseismology is more commonly based on coseismic subsidence (Dura *et al*., 2011; Nelson, Shennan, and Long, 1996;

Shennan *et al*., 2014). Coseismic subsidence is generally easier to capture, given that datable soil horizons are submerged and subsequently preserved by subtidal burial. Records of relative sea-level change are possible in areas that experience coseismic uplift (*e.g*., Atwater *et al*., 2004; Briggs *et al*., 2014; Sawai, 2001; Sawai and Nasu, 2005; Sawai *et al*., 2004), but only if long-term depositional subsidence or lateral progradation create the accommodation space necessary to preserve subsidence stratigraphy (Nelson, Kashima, and Bradley, 2009). Such a condition may be difficult to find along the Nicoya coastline, given the presence of long-term net tectonic emergence of the forearc (Marshall *et al*., 2012).

To explore the feasibility of obtaining a paleoseismic record from Nicoya, this study searched for suitable wetlands with intertidal sedimentary environments where recent relative sea-level changes might be recorded. Initially, possible wetlands were identified along the northern two-thirds of the outer Nicoya coastline using maps and satellite images (Figure 1b). Suitable wetlands are rare, given the small size of drainage basins on the narrow outer coast of the uplifting Nicoya forearc (Figure 1b). The depositional environments of four sites appeared promising. These sites were cored for basic stratigraphic characterization and age control, but the focus here was only on the two sites that yielded organic material suitable for radiocarbon dating.

The Tamarindo Estuary lies at the mouth of the 73 km^2 Matapalo basin (Battistini and Bergoeing, 1980) (Figure 1b). Although this estuary is located near the northern edge of the Nicoya segment and outside of the locked zone (Figure 1a), it also falls outside of the zone of significant permanent tectonic uplift (Marshall *et al*., 2012); therefore it is more likely to preserve subsidence stratigraphy. This site can be viewed as a test case for extracting a relative sea-level history from this environment, although the anticipated ground-level changes due to the seismic cycle (as defined by the last few hundred years only) are moderate (tens of centimeters). Although greater magnitude of uplift occurs farther south along the coastline, with a maximum observed in 2012 at Playa Carrillo (Protti *et al*., 2014), Tamarindo was selected for more intense study because the size of the wetland appeared more likely to yield prolonged subsidence stratigraphy that would be suitable for recording relative sea-level changes.

The ria-type (fluvial-formed), tide-dominated Tamarindo Estuary consists of a wide, sandy channel that is hypersaline during the dry season and isolated from the coast by a narrow, flat-topped peninsula that rises ~2.7 m above mean sea level (AMSL) (Figure 2a). Elevations reported here are based on surveying with level, rod, and laser range finder relative to mean sea level, defined as the midpoint between zero tide and mean high tides at Puntarenas, Costa Rica, the nearest tidal station. This peninsula is a beveled beach ridge, or chenier ridge, and is composed of semi-indurated, well-sorted, coarse, shell-rich sand (Figure 3). The estuary gives way to a broad, ecologically zoned mudflat wetland with a well-developed mangrove ecosystem (Figure 4). The mangroves grade from bank-forming (prop-root) *Rhizophora* trees (red mangrove) that surround the channel (Zone A; Figures 2b–c and 4) into brushier salt-resistant *Avicennia* (black mangrove) that extend into the broad mudflats beyond (Zones B and C; Figures 2b and 4). Clear mudflat patches, or salt flats, occur at supratidal to mean–high tide levels beyond the *Avicennia* zone (Zone D; Figures 2b, 2d, and 4). Zone D is hypersaline in the dry season (October through March) but can become flooded by fresh or brackish water during heavy rains of the wet season. The estuary itself varies in character. Along path BB′ (Figure 2a), the estuary consists of a broad, shallow, sandy-gravelly-shelly bottom with average local marine salinity (~32 parts per thousand [ppt]) (Figure 2e). Salinity gradually increases upstream in the channel due to evaporation, resulting in hypersaline conditions (>35 ppt) during the dry season. The channel abruptly narrows and transitions to a deeper, muddy bottom that is highly reduced and organic rich at the location shown in Figures 2a and 2e.

The transitions from subtidal reduced mud in the estuary channel, to lower-tidal *Rhizophora* peat, to upper-tidal *Avicennia* peat and mud, to oxidized mud of the upper salt flat

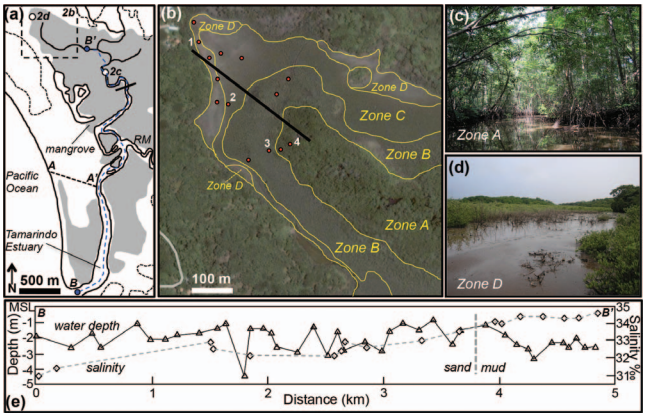

Figure 2. (a) Map of the Tamarindo Estuary. Gray area denotes the mangrove, intertidal environment. Dashed line represents 10 m contour (above sea level). Blue dashed line following the estuary from B to B′ indicates path taken for water/depth survey shown in Figure 2e. Dashed line AA′ indicates path surveyed for elevation profile across the sand peninsula in Figure 3. Box shows location seen in Figure 2b. Locations seen in photos in Figures 2c and 2d are shown by white dots (location in Figure 2d is 10.339°N, 85.844°W). The black line near marker 2d indicates where the estuary channel changes from a sandy, gravelly base (to the south) to a reduced, muddy channel (to the north), as depicted in Figure 2e. RM = Rio Matapalo. (b) Detailed eco-geomorphic map on a satellite image of the NW peripheral channel of the Tamarindo Estuary (location shown in Figure 2a). Zones refer to mangrove ecosystems: Zone A = *Rhizophora*, B = *Avicennia*, C = sparse *Avicennia*, D = open salt flat. Red circles are locations of cores. The line illustrates path for the ecoprofile shown in Figure 4. Numbered cores are shown in Figure 5. Satellite image is from Google Earth (point 1 = 10.3392° N, 85.8438° W). (c) Photograph of estuary channel in Zone A. Its location is shown in Figure 2a. This is the main channel of the estuary as surveyed in Figure 2e. The channel is several meters deep at low tide and has a reduced, muddy substrate. It has steep banks armored by prop-root mangroves. (d) Photograph of Zone D. Its location is shown in Figure 2a. The wet mud flat shown is hypersaline during the dry season, when it is inundated only by larger, near-spring tides. During the wet season it can also become a freshwater-runoff zone. (e) Profile of water depth relative to mean sea level and salinity of the estuary along path BB′, shown in Figure 2a. Dashed vertical gray line shows location of prominent transition from sandy, gravelly bottom to organic-rich, reduced, muddy bottom. (Color for this figure is available in the online version of this paper.)

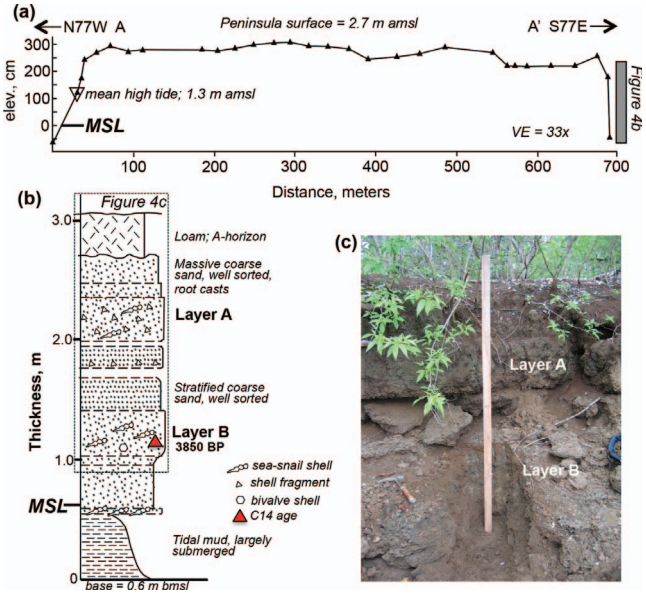

Figure 3. (a) Topographic profile based on leveling survey across the peninsula west of the Tamarindo Estuary along AA′ shown in Figure 2a. The peninsula is a raised sand berm that is on average 2.7 m AMSL and 1.4 m above the mean high tide. The surface tilts gently to the west, where it terminates at the estuary channel. (b) Stratigraphic column of the peninsula sand deposit, exposed at the estuary channel cut at A′ (Figure 2a) and denoted by the gray bar in Figure 3a. The entire sequence consists of coarse, well-sorted beach sand with common shells and shell fragments resting on a base of tidal mud. A shell from Layer B was dated to 3850 ±130 y BP (calibrated radiocarbon age; Table 1). (c) Photo of the upper part of exposure shown in Figure 3b. (Color for this figure is available in the online version of this paper.)

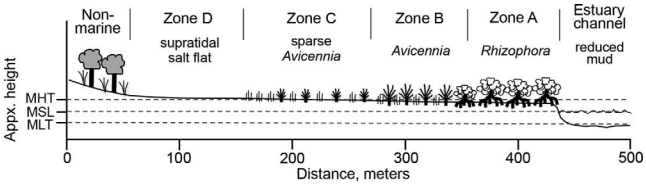

Figure 4. Schematic representation of the mangrove ecosystem at Tamarindo Estuary. Distances and elevations are approximate based on field inspection and not precise surveying. Schematic follows line shown in Figure 2b. Zones correspond to those shown in Figure 2b. MHT = mean high tide; MSL = mean sea level; MLT = mean low tide.

(Figure 4) are consistent with the expected zonation of mangroves as lying between mean sea level and highest astronomical tide (Belperio, Harvey, and Bourman, 2002; Ellison, 2008; Grand Pre *et al*., 2012; Ramcharan and McAndrews, 2006; Rowe, 2007; Saintilan and Hashimoto, 1999). Although a detailed topographic survey along the profile in Figure 4 has not been completed, observations show that the supratidal salt flat (Zone D) is flooded by tidal sheetflow only at spring tide conditions. A leveling line survey from Zone D to the outer beach *via* roads did imply a lower elevation than highest tide. This suggests the possibility that tidal currents are slowed by the narrow estuary channel and drag in the mangrove, and they do not reach as high elevation in the tidal flats as along the open shoreface. It is also possible that Zone D elevation is slightly lower than the more seaward zones (*e.g*., Zones 2 and 3), either due to subsidence associated with shrinking during the dry season or due to formation of retarding levies *via* either sedimentation or anthropogenic activity related to prehistoric saltworks in the estuary.

The Tamarindo Estuary contains geomorphic evidence for Holocene sea-level change. A stand of dead and dying non-mangrove trees at the northern edge of the estuary suggests recent (but pre-2012) relative sea-level rise, possibly associated with post-1950 interseismic subsidence. The lagoon barrier implies earlier relative sea-level fall. The 2.7 m AMSL beveled beach ridge may have been deposited during a mid- to late-Holocene highstand. Although regional records suggest that sea level stabilized near present levels by about 5000 years BP (Caballero *et al*., 2005; Curray, Emmel, and Crampton, 1969; Fleming *et al*., 1998; Sirkin, 1985), sea level just prior to this may have been a highstand of several meters above modern levels. This is suggested by global records of sea level in the tropics and models of sea-level change that take into account ocean siphoning near the equator due to glacio-isostatic adjustment (Milne and Mitrovica, 2008; Mitrovica and Milne, 2002). One radiocarbon age obtained from a shell in this sand of 3850 ±130 years BP (calibrated age; see Table 1, Figure 3) does imply that the beach ridge postdates the glacio-isostatic highstand. However, storm overwash or tectonic uplift may have also contributed to the height of this beach ridge.

The upper Tamarindo mudflat was cored in 2010 and 2011, using both gouge (2.5 cm diameter) and Russian-type (6 cm diameter) borers, to define recent depositional history and test for cyclic relative sea-level changes that may relate to earthquake history. This study hypothesized that sea-level change would be recorded by lateral migration of tidal mangrove zones. Specifically, coseismic uplift might result in emergence of the reduced subtidal muds of the estuary channel, over which mangrove peats might form. Coseismic uplift in temperate estuaries has been documented by freshwater peats developed over tidal mud with very sharp contacts (Atwater *et al*., 2004; Sawai *et al*., 2004). Similarly, oxidized salt flats and paleosols might form atop mangrove peats that were uplifted too far out of the intertidal zone. The primary goals for this coring effort were as follows: (1) assess whether coherent stratigraphy existed in this heavily bioturbated environment; (2) quantify depositional history and assess whether the age of deposits would overlap with the late-Holocene earthquake history; (3) test whether alternating facies are present that could indicate a history of relative sea-level changes; and (4) document lithostratigraphy and qualitatively interpret facies changes (recognizing that quantitative relative sea-level history would require future biostratigraphic work).

The second site, Playa Carrillo, is located along the central Nicoya coast (Figure 1b), above the locked zone of the megathrust (Feng *et al*., 2012) and centered in the zone of greatest coseismic uplift (0.7 m) during the 2012 earthquake

Table 1. *Radiocarbon data*.

Core	Depth (cm)	ID	Lab	Material	$\delta^{13}C$ (per mil)	^{14}C Age, y BP (1σ)	Calibrated Age, y BP (95%)	Median (y BP)
Car	149	Carrillo-2-149	UGA-9387	plant fragment	−28.0	140 +20	172–231	202
Car	176	Carrillo-1-176	UGA-9386	plant fragment	−28.4	400 +20	447–508	478
1	41	X3A2#2	Beta-278009	organic sediment	−24.8	720 +40	650–700	675
1	55	X3A2#3	Beta-278010	organic sediment	−23.1	1160 +40	970–1180	1075
1	63	X3A2#4	Beta-278011	organic sediment	−23.6	1640 +40	1420–1620	1520
Exp	180	CR10-01	Beta-283107	shell	+3.1	4130 +40	3720–3980	3850
4	282	CRRHIZ282	UGA-9382	plant fragment	−26.3	3910 +30	4280–4421	4351
2	89	X11#1	Beta-278016	plant fragment	−27.7	4070 +40	4430–4650	4540
2	107	X7#3	Beta-278015	plant fragment	−26.8	4590 +40	5280–5330	5305
2	179	X7#1	Beta-278013	plant fragment	−26.7	4640 +40	5300–5470	5385
4	222	CRRHIZ222	UGA-9383	plant fragment	−29.5	5070 +25	5746–5834	5790
3	273	CRAVIC273	UGA-9384	plant fragment	−27.4	5560 +25	6301–6399	6350
2	141	X7#2	Beta-278014	plant fragment	−28.1	5780 +40	6480–6670	6575
4	358	CRRHIZ358	UGA-7545	plant fragment	−26.6	5970 +25	6740–6882	6810
3	351	CRAVIC351	UGA-7543	plant fragment	−26.6	6330 ±25	7236–7316	7275
3	371	CRAVIC371	UGA-7544	plant fragment	−27.0	6360 +25	7249–7332	7290

Ages are listed in order of increasing median calibrated age, which correspond to ages reported on other figures. All ages were measured using AMS. Dates are reported in y BP relative to 1950. ^{14}C age is the conventional radiocarbon age, which is the measured age corrected for isotopic fractionation. Calibrated ages from Beta Analytic are based on INTCAL04. Calibrated ages from UGA are based on INTCAL09.14c. Depth relative to top of exposure shown in Figure 4.

Abbreviations: Car = Carrillo site, Exp = exposure of sand at Tamarindo, UGA = University of Georgia, Beta = Beta Analytic.

(Protti *et al*., 2014). The site consists of a small wetland in a valley that may have once hosted the Ora River (Morrish *et al*., 2009). Topography suggests that the Ora River was captured by a coastal tributary eroding headwardly from the SW. Although the current drainage area of this wetland is small, the local depositional setting seemed promising for recording the recent relative sea-level change. The wetland surface was 1.2 m AMSL when cored in 2011 (prior to coseismic uplift) and thus prone to shallow flooding during monthly spring tides, and it was separated from the foreshore by an aggrading berm sequence (beach ridge) lying ∼2.5 m AMSL. One reconnaissance core was obtained from this site.

All cores from these sites were described in the field. Age control was established using 15 accelerator mass spectrometry (AMS) radiocarbon ages using both Beta Analytic and the Center for Applied Isotope Studies at the University of Georgia (UGA) (Table 1). Ages are reported as calibrated ages relative to 1950 and were calibrated using IntCal04 (for Beta Analytic ages; Reimer *et al.,* 2004) and IntCal09.14c (for UGA ages; Reimer, *et al.,* 2009). Radiocarbon ages were obtained on plant/wood fragments or bulk organic material (Table 1). The wood fragments typically consisted of reddish-brown pieces up to several centimeters in diameter that appeared detrital and lacked surface features typical of roots. Although it is possible that large wood fragments can be transported large distances and thus have long residence time prior to burial, this study interprets these wood fragments to have been derived locally from dead mangrove limbs that were transported only a short distance prior to deposition in the mangrove swamp. Therefore, one can expect the residence times at the surface prior to burial to have been minimal relative to the burial ages. This interpretation is speculative, however, given that the possibility of unique identification of the fragments as sourced from proximal mangrove trees does not exist and that there is no corroborating taphonomic evidence for how long they could survive prior to burial. Given that ages from wood fragments overlap with bulk sediment ages, and given that the burial ages are mostly old, these assumptions seem reasonable for our reconnaissance efforts.

RESULTS

This study focused investigations at Tamarindo at the northern tip of one peripheral estuarine channel, where an easily accessed transition in mangrove zones occurs over several hundred meters (Figure 2b). Fourteen cores were collected, ranging from 2–4 m depth, from the different mangrove eco-zones. Logs of representative cores from each zone are shown in Figure 5. The recovered stratigraphy was variable and generally could not be correlated between widely (>10 m) spaced cores. Repeat cores at individual locations ∼1 m apart, however, did reveal coherency. Such lateral variation is not uncommon for mangrove wetlands, where lateral variations in compaction, depositional environment, and preexisting topography are typical (Belperio, Harvey, and Bourman, 2002; Berkeley *et al*., 2009; Dura *et al*., 2011). Primary depositional features were also poorly preserved in cores, likely due to bioturbation and slow burial (see below).

The open tidal flat (Zone D) exhibits the most variable and laterally discontinuous stratigraphy (Figure 5). The upper meter consists of interbedded mud and sandy mud, which could have been deposited in an evolving salt flat above mean tide level. These horizons are heavily bioturbated, partially oxidized, gradational, and complex. Below these layers, a thicker layer of hard, greenish-gray, silty clay occurs, which was interpreted to be a deposit layer in a submerged tidal flat. This transition at ∼1 m depth may indicate minor emergence (relative sea-level fall) in the more recent depositional history.

Stratigraphy in the vegetated *Avicennia* and *Rhizophora* mangrove eco-zones (Zones A, B, and C) is more continuous, generally consisting of gray and brown silty clay in ∼25 cm thick, bioturbated layers overlying a prominent transition to soft, silty peat at ∼1–1.4 m depth (Figure 5). The dark peat

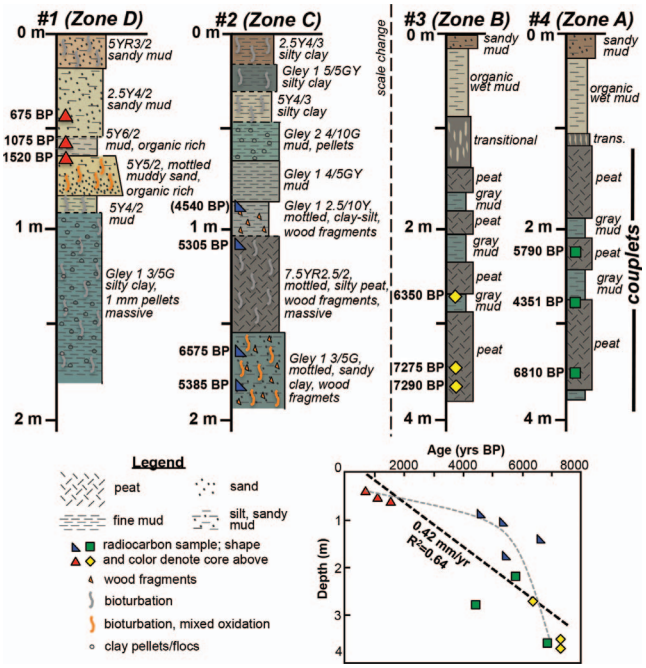

Figure 5. Stratigraphy of four representative cores from Tamarindo. Location of cores is shown in Figure 2. The vertical scale changes from left to right. Surface (0 m) is approximately at mean high-tide level. All core sites are estimated to be within ~0.2 m elevation of each other, although a precise survey was not completed. Legend shown at bottom left. Colors are approximately the colors of horizons observed in the field. Colored shapes represent calibrated radiocarbon ages (median of 2σ range for most prominent peak) in years before present (BP) relative to 1950 (see Table 1). The 4540 BP age in Core 2 is extrapolated from a nearby core. Ages are plotted versus depth for all cores in the lower right, defining an average depositional age of 0.4 mm/y. The light dashed line illustrates the potential nonlinear deposition rate involving rapid early-Holocene filling and deceleration toward the present. (Color for this figure is available in the online version of this paper.)

contains large, red wood fragments and other herbaceous debris with an estimated organic content of more than 20%, which we interpret to be derived from prop-root type mangrove trees of the *Rhizophora* eco-zone. This is consistent with observations and descriptions in other similar environments (Grand Pre *et al.*, 2012). Prop-root type mangroves generally form peats when above mean high-tide level, suggesting a history of relative sea-level rise over the span of the cores (Belperio, Harvey, and Bourman, 2002; Dura *et al.*, 2011; Ellison, 2008; Engelhart et al., 2007; Grand Pre *et al.*, 2012; Ramcharan and McAndrews, 2006; Rowe, 2007; Saintilan and Hashimoto, 1999). Interbedded with the peat are 10–15 cm thick horizons of featureless gray-green mud, which could not be correlated between cores. The alternation of peat and mud is more pronounced below 1.5 m depth and continues to the maximum core depth of 4 m. The lack of extensive organic debris and the reduced nature of these muds is consistent with deposition in a consistently submerged environment well below mean tide level, such was observed in the modern environment in the base of the estuary channel. The alternations between mud (subtidal) and peat (higher than mean tide) may indicate cyclic relative sea-level change during the longer history of submergence recorded below 1 m depth. In contrast, the lack of gray mud and peat in the upper meter of cores implies deposition above the prop-root eco-zone in the marginal mangrove system (*e.g.*, Zone D). This interpretation is consistent with the degree of partial oxidation and complexity resulting from bioturbation in the upper meter, which are suggestive of periodic subaerial exposure.

Calibrated AMS radiocarbon ages (relative to 1950) are shown on cores and plotted in the lower right of Figure 5. Errors on ages (not shown) are generally ±100 years for the main calibrated peak (specific ranges provided in Table 1). Ages range from 675–7290 years BP. The antiquity of the upper meter of sediment is corroborated by a pottery shard from 0.7 m depth in Zone D (Core 1), which displays markings typical of pottery, tools, and artworks common to the middle first millennium (AD) pre-Columbian Costa Rican culture (Fernandez and Alvarado, 2006). Ages correlate roughly with depth, implying an average depositional rate of ~0.4 mm/y, although there are individual ages in Cores 2 and 4 that fall out of depositional sequence (Figure 5; Table 1). This may indicate that inheritance is a problem in some ages obtained from wood fragments. Given the overall trend and the overlap between ages measured on wood fragments and bulk sediment, however, the age control for these cores should provide at least an approximation of overall Holocene depositional history of the estuary. Nonetheless, the weakness of the trend and the apparent age variation between cores suggests complexity that would require additional dating to fully characterize. For example, given the uncertainty in the age-depth trend, it is possible that deposition slowed toward the present following a more rapid interval of early to mid-Holocene accretion (Figure 5).

The reconnaissance core and radiocarbon ages from Playa Carrillo indicate a different depositional history than observed at Tamarindo (Figure 6). Although Carrillo currently has a much smaller drainage area and should thus have lower sedimentation rate, the basal date of 470 years BP suggests a depositional rate of 3.7 mm/y, seven times faster than at Tamarindo. The stratigraphy of this site is also different, consisting mainly of brown sand in the upper 1.2 m, with a mixture of gray sand and muddy sand mixed with peat below. The sands contain abundant shell fragments, including well-preserved *Turritella* gastropods (sea-snail shells) that are common in the swash zone of the foreshore beach environment. The sand horizons were generally not thin or well enough sorted to indicate deposition by tsunami. These observations imply a transition from a generally submerged intertidal mangrove environment to sand produced by rapid infilling by overwash from the beach across the storm berm (*e.g.*, Wang and Horwitz, 2007) or sand in-wash transported from the estuary during highest tide (Figure 6).

DISCUSSION

The age of the deposits at the Tamarindo Estuary likely preclude this site from being useful for recording events over the past few thousand years. The average depositional rate of 0.4 mm/y implies that the transition in facies associated with frequent megathrust ruptures (as known from the historical

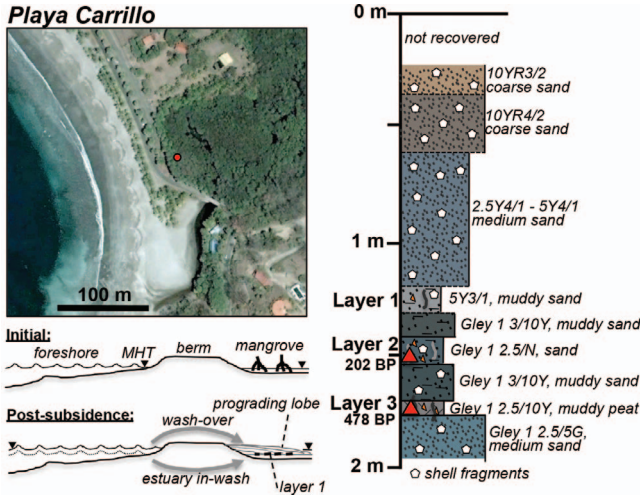

Figure 6. Reconnaissance of Playa Carrillo site. Upper left shows Google Earth satellite image (pre-2012) of the estuary; dot indicates core location (9.8672° N, 85.4826° W). Stratigraphy of core is shown to the right, using same symbols as in Figure 5. Ground surface elevation (0 m) was approximately 1.2 m AMSL when core was taken in 2011 (prior to uplift during the 2012 earthquake). The lower left shows conceptual cross sections explaining how the sand deposited above Layer 1 may result from subsidence of the berm and washover from the foreshore environment or tidal in-wash from the estuary. MHT = mean high tide, denoted by triangle. (Color for this figure is available in the online version of this paper.)

record) may occur over just a few centimeters of stratigraphy, which could be too narrow to be preserved given the extent of bioturbation. The signal-to-noise ratio may thus be too low to constrain ground-level fluctuations associated with the most recent (including historic) interplate earthquakes.

The earlier history preserved in this estuary appears to record regional relative sea-level changes. The occurrence of peats below 1 m depth suggests relative sea-level rise on the order of 2–3 m between 7300 and 4500 years BP. Regional sea-level rise during this same period was likely on the order of several meters, followed by sea-level stabilization by ~5000 years BP (Caballero *et al*., 2005; Curray, Emmel, and Crampton, 1969; Fleming *et al*., 1998; Sirkin, 1985) or even a highstand at about the same time (Milne and Mitrovica, 2008; Mitrovica and Milne, 2002), suggesting that the submergence of these soil horizons may have been due to regional sea-level change and that the coast during this period did not experience appreciable tectonic uplift or subsidence. A similar pattern has been observed in numerous other tropical mangrove environments, where coring has revealed early to mid-Holocene infilling associated with regional sea-level rise (*i.e*. a transgressive lithologic sequence) followed by slower deposition since 5–7 ka (Belperio, Harvey, and Bourman, 2002; Dura *et al*., 2011; Grand Pre *et al*., 2012; Rowe, 2007). The transition in the cores from reduced mud to oxidized, bioturbated mud in the salt flat (Zone D) may in turn represent relative sea-level drop following a mid- to late-Holocene highstand, with transition from a tidal to a supratidal environment. The record at Tamarindo thus implies no major permanent tectonic uplift during the middle to late Holocene, because it would need to have been balanced by a comparable magnitude of deposition-related subsidence that would not be expected from such a small basin.

The cyclic relative sea-level changes indicated by the peat-mud alternations below 1 m depth could, however, reflect moderate uplift/subsidence events related to paleoearthquakes and the megathrust seismic cycle that were imposed on the transgressive sequence. Because these alternations could be formed by other dynamic factors in the mangrove depositional environment, such as channel migration, it cannot yet be concluded that they represent paleoearthquakes. Additional work is necessary, including more-closely spaced cores to rule out lateral depositional changes, higher resolution dating, and micropaleontological biostratigraphic analysis (*e.g*., Hemphill-Haley, 1995; Horton *et al*., 2007; Dura *et al*., 2011; Sawai, 2001; Sawai, Horton, and Nagumo, 2004; Sawai *et al*, 2004; Shennan *et al*., 2014; Sherrod, 1999). For example, Grand Pre *et al*. (2012) were able to demonstrate that a peat-mud transition represented a solitary early-Holocene coseismic subsidence event in a similar mangrove environment along the Sunda megathrust in Indonesia. A potential problem at this study's site is that the possible recurrence time based on historical observations (~50 y) is so short that the marsh depositional environment may not have time to reset before the seismic cycle is repeated; determining whether it is requires further testing. Another limitation at Tamarindo is that there are no obvious sedimentary indicators of tsunami inundation, whereas tsunamis are key aspects of paleoseismic records at other sites of similar depositional environment (*e.g*., Ramirez-Herrera *et al.,* 2014).

Due to its younger depositional history, Playa Carrillo is better suited for recording more recent relative sea-level changes, possibly connecting stratigraphy to the historical earthquake record. It was interpreted that the upper 1.2 m of sand at Carrillo was deposited recently (in the past 100 y?) *via* overwash from the beach zone (*e.g*., Wang and Horwitz, 2007) or *via* the estuary during storms. Additional ages (*e.g*., from Layer 1; Figure 6) would be required to better constrain the timing of this deposition. Infilling and progradation of sand may have been facilitated by interseismic subsidence, as the beach ridge gradually lowered relative to the high-water levels of storms and highest astronomical tides. Beneath the sand, the bioturbated, gray, muddy sand horizon (Layer 1) may be a buried soil horizon. Although not a peat, the wood fragments may indicate deposition in the high mangrove zone (*i.e*. above mean high tide), whereas this horizon was at mean sea level prior to uplift in the 2012 earthquake. It is possible that this layer was deposited after emergence associated with the penultimate event (*i.e*. 1950). The peat-mud alternations below this could in turn represent earlier uplift events followed by gradual subsidence and burial. If true, some previous events may not be preserved, given that the historical record documents three events in the past 200 years prior to 2012 (Protti *et al*., 2014), whereas the deepest muddy peat in the core (Layer 3) was deposited ~480 years BP. Better age control of these couplets is required to further test this hypothesis. It is also uncertain how far back this record may go, given that we did not attempt deeper cores at this site.

These investigations should be considered reconnaissance in nature, given the limited spatial distribution of cores, uncer-

tainties in age constraints, and the lack of biostratigraphic analysis. Preliminary results suggest that viable paleoseismic sites may be present along the Nicoya segment of the Middle America Trench, but that they are likely rare and have complex and fragmented records. Due to slow deposition, Tamarindo does not preserve a record of the most recent events, although older peat-mud alternations may represent mid-Holocene megathrust earthquakes. In contrast, historical events may be recorded by younger sediment at Carrillo, but the record may be fragmentary (*i.e.* missing events) and it is unclear how far back it extends. The Carrillo site illustrates the potential of localized depositional settings for recording a paleoseismic signal, suggesting that the search for sites should go beyond obvious, large estuaries and wetlands. This is important, given the relative rarity of large wetlands along the peninsula, due to tectonic emergence, wave energy, and coastline and drainage basin geometry. One site not yet investigated which has potential given similarity to Carrillo is the Bongo River Estuary (Figure 1b). Likewise, one major wetland not yet explored that could have a potential paleoseismic record is the estuary of the Tempisque River in the Gulf of Nicoya, although this may be too far from the trench to experience significant earthquake-related relative sea-level change.

The complexity of deposits that were observed in this study shows the importance of including biostratigraphic analysis in future work. It is well known that biostratigraphic proxies have the potential to document higher-resolution records of relative sea-level changes. Vertical zonation of intertidal facies at the decimeter scale in both temperate and tropical environments can be deciphered using local assemblages of diatoms (Hemphill-Haley, 1995; Sawai, 2001; Sawai, Horton, and Nagumo, 2004; Sherrod, 1999), foraminifera (Belperio, Harvey, and Bourman, 2002; Berkeley *et al*., 2009; Horton *et al*., 2007), or pollen (Ellison, 2008; Engelhart *et al*., 2007; Rashid *et al*., 2013; Rowe *et al*., 2007). These paleoenvironmental indicators can be highly sensitive to coastal gradients in salinity and other variables, enabling construction of transfer functions that quantitatively relate proxy assemblages to depositional water elevation (Grand Pre *et al*., 2012; Horton *et al*., 2007). Application of these techniques to Nicoya sites where suitable stratigraphy is present, such as at Carrillo, may prove fruitful for constraining the paleoseismic history of this megathrust.

CONCLUSIONS

This study has identified potential paleoseismic sites along the Nicoya segment of the Middle America megathrust at Tamarindo and Playa Carrillo. Due to the nature of the Nicoya coastline, potential sites with suitable subsidence stratigraphy are rare. At Tamarindo, estuary sedimentation related to overall early-Holocene sea-level rise records lithostratigraphic changes that may relate to minor relative sea-level change associated with subduction zone earthquakes. Late-Holocene events do not appear to be preserved, however, given slow deposition after ~5 ka. Younger stratigraphy is exhibited at the Playa Carrillo Estuary, including peat-mud alternations that may represent relative sea-level changes associated with subduction zone earthquakes over the past 500 years. More coring, environmental analysis, and chronostratigraphy are required to constrain these events, however. In addition, biostratigraphy is required at both sites to enable quantitative interpretation of relative sea-level history. Although these results suggest a paleoseismic record is preserved along the Nicoya coastline, this record appears fragmented and will require careful additional work at numerous sites to patch together a coherent history.

ACKNOWLEDGMENTS

The following people and organizations are thanked for assistance with this work: Alyssa Durden, Craig Cunningham, Illiya Smithka, Shawn Morrish, Lewis Owen, Bibi Santidrian, Gabriel Blanco, Ken Lacovara, Marino Protti, Mario Boza, Las Baulas National Marine Park, and the Leatherback Trust. Brian Atwater and anonymous reviewers are thanked for their reviews of an earlier version of this manuscript. Funding for this research was provided by MARGINS/NSF: OCE0948290.

LITERATURE CITED

Atwater, B.F., 1987. Evidence for great Holocene earthquakes along the outer coast of Washington state. *Science,* 236(4804), 942–944.

Atwater, B.F.; Kurukawa, R.; Hemphill-Haley, E.; Ikeda, Y.; Kashima, K.; Kawase, K.; Kelsey, H.; Moore, A.; Nanayama, F.; Nishimura, Y.; Odagiri, S.; Ota, Y.; Park, S.; Satake, K.; Sawai, Y., and Shimokawa, K., 2004. Seventeenth-century uplift in Eastern Hokkaido, Japan. *The Holocene,* 14(4), 487–501.

Audet, P. and Schwartz, S., 2013. Hydrologic control of forearc strength and seismicity in the Costa Rican subduction zone. *Nature Geoscience,* 6(10), 852–855.

Battistini, R. and Bergoeing, J.P., 1980. Caracteristicas geomorfologicas del litoral comprendido entre Bahia de Tamarindo y Bahia Culebra, Peninsula de Nicoya, Costa Rica. *Revista Geografica,* 98, 79–90.

Belperio, A.; Harvey, N., and Bourman, R., 2002. Spatial and temporal variability in the Holocene sea-level record of the South Australian coastline. *Sedimentary Geology,* 150(1–2), 153–169.

Berkeley, A.; Perry, C.; Smithers, S.; Horton, B., and Cundy, A., 2009. Foraminiferal biofacies across mangrove-mudflat environments at Cocoa Creek, north Queensland, Australia. *Marine Geology,* 263(1–4), 64–86.

Bilek, S.L.; Schwartz, S.Y., and DeShon, H.R., 2003. Control of seafloor roughness on earthquake rupture behavior. *Geology,* 31(5), 455–458.

Briggs, R.W.; Engelhart, S.; Nelson, A.; Dura, T.; Kemp, A.; Haeussler, P.; Corbett, D.; Angster, S., and Bradley, L., 2014. Uplift and subsidence reveal a nonpersistent megathrust rupture boundary (Sitkinak Island, Alaska). *Geophysical Research Letters,* 41(7), 2289–2296.

Caballero, M.; Peñalba, M.C.; Martínez, M.; Ortega-Guerrero, B., and Vázquez, L., 2005. A Holocene record from a former coastal lagoon in Bahía Kino, Gulf of California, Mexico. *The Holocene,* 15(8), 1236–1244.

Carver, G.A. and McCalpin, J.P., 1996. Paleoseismology of compressional tectonic environments. *In:* McCalpin, J.P. (ed.), *Paleoseismology*. New York: Academic, pp. 183–270.

Cisternas, M.; Atwater, B.; Torrejon, F.; Sawai, Y.; Machuca, G.; Lagos, M.; Eipert, A.; Youlton, C.; Salgado, I.; Kamataki, T.; Shishikura, M.; Rajendran, C.; Malik, J.; Rizal, Y., and Husni, M., 2005. Predecessors of the giant 1960 Chile earthquake. *Nature,* 437(7057), 404–407.

Curray, J.R.; Emmel, F.J., and Crampton, P.J.S., 1969. Holocene history of a strand plain lagoonal coast, Nayarit, Mexico. *Proceedings of Lagunas Costeras, Un Simposio, Memorias Simposio Internacional* (Mexico City, Mexico, UNAM-UNESCO), pp. 63–100 [in Spanish].

DeMets, C.; Gordon, R.G., and Argus, D.F., 2010. Geologically current plate motions. *Geophysical Journal International,* 181(1), 1–80.

DeShon, H.R.; Schwartz, S.Y.; Newman, A.V.; González, V.; Protti, M.; Dorman, L.M.; Dixon, T.H.; Sampson, D.E., and Flueh, E.R., 2006. Seismogenic zone structure beneath the Nicoya Peninsula, Costa Rica, from three-dimensional local earthquake P- and S-wave tomography. *Geophysical Journal International,* 164(1), 109–124.

Dura, T.; Rubin, C.; Kelsey, H.; Horton, B.; Hawkes, A.; Vane, C.; Daryono, M.; Grand Pre, C.; Ladinsky, T., and Bradley, S., 2011. Stratigraphic record of Holocene coseismic subsidence, Padang, West Sumatra. *Journal of Geophysical Research,* 116(B11), B11306. doi:10.1029/2011JB008205

Ellison, J.C., 2008. Long-term retrospection on mangrove development using sediment cores and pollen analysis: A review. *Aquatic Botany,* 89(2), 93–104.

Engelhart, S.E.; Horton, B.; Roberts, D.; Bryant, C., and Corbett, D., 2007. Mangrove pollen of Indonesia and its suitability as a sea-level indicator. *Marine Geology,* 242(1), 65–81.

Feng, L.; Newman, A.; Protti, M.; Gonzalez, V.; Jiang, Y., and Dixon, T., 2012. Active deformation near the Nicoya Peninsula, northwestern Costa Rica, between 1996 and 2010: Interseismic megathrust coupling. *Journal of Geophysical Research,* 117(B6), B06407. doi:10.1029/2012JB009230

Fernandez, P. and Alvarado, G.E., 2006. *Artesanso y piedras: Herramientas y escultura precolumbina en Costa Rica*. San Jose, Costa Rica: Central Bank Museums Foundation of Costa Rica, 128p.

Fisher, D.; Gardner, T.; Marshall, J.; Sak, P., and Protti, M., 1998. Effect of subducting sea-floor roughness on forearc kinematics, Pacific coast, Costa Rica. *Geology,* 26(5), 467–470.

Fleming, K.; Johnston, P.; Zwartz, D.; Yokoyama, Y.; Lambeck, K., and Chappell, J., 1998. Refining the eustatic sea-level curve since the Last Glacial Maximum using far and intermediate sites. *Earth and Planet. Science Letters,* 163(1), 327–342.

Grand Pre, C.A.G.; Horton, B.; Kelsey, H.; Rubin, C.; Hawkes, A.; Daryono, M.; Rosenberg, G., and Culver, S., 2012. Stratigraphic evidence for an early Holocene earthquake in Aceh, Indonesia. *Quaternary Science Reviews,* 54, 142–151.

Hemphill-Haley, E., 1995. Diatom evidence for earthquake-induced subsidence and tsunami, Washington. *Geological Society of America Bulletin,* 107(3), 367–378.

Horton, B.P.; Culver, S.; Hardbattle, M.; Larcombe, P.; Milne, G.; Morigi, C.; Whittaker, J., and Woodroffe, S., 2007. Reconstructing Holocene sea-level change for the central Great Barrier Reef (Australia) using subtidal foraminifera. *Journal of Foraminiferal Research,* 37(4), 327–343.

Hyndman, R. and Wang, K., 1993. Thermal constraints on the zone of major thrust earthquake failure: The Cascadia subduction zone. *Journal of Geophysical Research,* 98(B2), 2039–2060.

Iinuma, T.; Protti, M.; Obana, K.; Gonzalez, V.; Van der Laat, R.; Kato, T.; Miyazaki, S.; Kaneda, Y., and Hernandez, E., 2004. Interplate coupling in the Nicoya Peninsula, Costa Rica, as deduced from a trans-peninsula GPS experiment. *Earth and Planetary Science Letters,* 223(1), 203–212.

Jankaew, K.; Atwater, B.; Sawai, Y.; Choowong, M.; Charoentitirat, Y.; Martin, M., and Prendergast, A., 2008. Medieval forewarning of the 2004 Indian Ocean tsunami in Thailand. *Nature,* 455(7217), 1228–1231.

Kinoshita, M.; Moore, G.; von Huene, R.; Tobin, H., and Ranero, C., 2006. The seismogenic zone experiment. *Oceanography,* 19(4), 28–38.

MARGINS Staff, 2004. *Science Plans*. Washington, D.C.: National Science Foundation, MARGINS Office, 159p.

Marshall, J.S. and Anderson, R., 1995. Quaternary uplift and seismic cycle deformation, Península de Nicoya, Costa Rica. *Geological Society of America Bulletin,* 107(4), 463–473.

Marshall, J.S.; Morrish, S.; LaFromboise, E.; Butcher, A.; Ritzinger, B.; Wellington, K.; Barnhart, A.; Kinder, K.; Utick, J.; Protti, M.; Gardner, T.; Fisher, D.; Simila, G.; Spotila, J.; Owen, L.; Murari, M., and Cupper, M., 2012. Morphotectonic segmentation along the Nicoya Peninsula seismic gap, Costa Rica, Central America. *Seismological Research Letters,* 83(2), 374.

McCaffrey, R., 2008. Global frequency of magnitude 9 earthquakes. *Geology,* 36(3), 263–266.

Milne, G.A., and Mitrovica, J.X., 2008. Searching for eustasy in deglacial sea-level histories. *Quaternary Science Reviews,* 27(25), 2292–2302.

Mitrovica, J.X., and Milne, G.A., 2002. On the origin of late Holocene sea-level highstands within equatorial ocean basins. *Quaternary Science Reviews,* 21(20), 2179–2190.

Monecke, K.; Finger, W.; Klarer, D.; Kongko, W.; McAdoo, B.; Moore, A., and Sundrajat, S., 2008. A 1,000-year sediment record of tsunami recurrence in northern Sumatra. *Nature,* 455(7217), 1232–1234.

Morrish, S.; Marshall, J.; LaFromboise, E.; Utick, J.; Piestrzeniewicz, P., and Protti, M., 2009. Coastal uplift and stream piracy as indicators of net seismic cycle deformation along the Costa Rica Pacific margin: Puerto Carrillo Headland and Rio Ora Valley, Nicoya Peninsula. *In: Geological Society of America, 2009 Annual Meeting, Abstracts with Programs, 41(7)*. Boulder, Colorado: Geological Society of America, p. 674.

Nelson, A.R.; Kashima, K., and Bradley, L., 2009. Fragmentary evidence of great-earthquake subsidence during Holocene emergence, Valdivia Estuary, South Central Chile. *Bulletin of the Seismological Society of America,* 99(1), 71–86.

Nelson, A.R.; Shennan, I., and Long, A.J., 1996. Identifying coseismic subsidence in tidal-wetland stratigraphic sequences at the Cascadia subduction zone of western North America. *Journal of Geophysical Research,* 101(B3), 6115–6135.

Newman, A.; Schwartz, S.; Gonzalez, V.; DeShon, H.; Protti, M., and Dorman, L., 2002. Along strike variability in the seismogenic zone below Nicoya Peninsula, Costa Rica. *Geophysical Research Letters,* 29(20). doi:10.1029/2002GL015409

Nishenko, S.P., 1989. Circum-Pacific Seismic Potential, 1989–1999. *U.S. Geological Survey Open File Report 89-0086,* 126p.

Norabuena, E.; Dixon, T.; Schwartz, S.; DeShon, H.; Newman, A.; Protti, M.; Gonzalez, V.; Dorman, L.; Flueh, E.; Lundgren, P.; Pollitz, F., and Sampson, D., 2004. Geodetic and seismic constraints on some seismogenic processes in Costa Rica. *Journal of Geophysical Research,* 109(B11), B11403. doi:10.1029/2003JB002931

Protti, M.; Gonzalez, V.; Newman, A.; Dixon, T.; Schwartz, S.; Marshall, J.; Feng, L.; Walter, J.; Malservisi, R., and Owen, S., 2014. Nicoya earthquake rupture anticipated by geodetic measurement of the locked plate interface. *Nature Geoscience,* 7(2), 117–121.

Protti, M.; Guendel, F., and Malavassi, E., 2001. *Evaluación del Potencial Sísmico de la Península de Nicoya*, 1st edition. Heredia, Costa Rica: Editorial Fundación Universidad Nacional Autónoma, 144p.

Protti, M.; Guendel, F., and McNally, K., 1995. Correlation between the age of the subducting Cocos plate and the geometry of the Wadati-Benioff zone under Nicaragua and Costa Rica. *In:* Mann, P. (ed.), *Geologic and Tectonic Development of the Caribbean Plate Boundary in Southern Central America*. Boulder, Colorado: Geological Society of America Special Paper No. 295, pp. 309–326.

Ramcharan, E. and McAndrews, J., 2006. Holocene development of coastal wetland at Maracas Bay, Trinidad, West Indies. *Journal of Coastal Research,* 22(3), 581–585.

Ramirez-Herrera, M.T.; Corona, N.; Lagos, M.; Cerny, J.; Goguitchaichvili, A.; Goff, J.; Cague-Goff, C.; Machain, M.; Zawadzki, A.; Jacobsen, G.; Carranza-Edwards, A.; Lozano, S., and Blecher, L., 2014. Unearthing earthquakes and their tsunamis using multiple proxies: The 22 June 1932 event and a probably fourteenth-century predecessor on the Pacific coast of Mexico. *International Geology Review,* 53(13). doi:10.1080/00206814.2014.951977

Rashid, T.; Suzuki, S.; Sato, H.; Monsur, M., and Saha, S., 2013. Relative sea-level changes during the Holocene in Bangladesh. *Journal of Asian Earth Sciences,* 64, 136–150.

Reimer, R.J.; Baille, M.; Bard, E.; Bayliss, A.; Beck, J.; Bertrand, C.; Blackwell, P.; Buck, C.; Burr, B.; Cutler, K.; Damon, P.; Edwards, R.; Fairbanks, R.; Friedrich, M.; Guilderson, T.; Hogg, A.; Hughen, K.; Kromer, B.; McCormac, G.; Manning, S.; Ramsey, C.; Reimer, R.; Remmele, S.; Southon, J.; Stuiver, M.; Talamo, S.; Taylor, F.;

van der Plicht, J., and Weyhenmeyer, C., 2004. IntCal04 terrestrial radiocarbon age calibration, 0–26 cal kyr B.P. *Radiocarbon*, 46(3), 1029–1058.

Reimer, P.J.; Baillie, M.; Bard, E.; Bayliss, A.; Beck, J.; Blackwell, P.; Ramsey, C.; Buck, C.; Burr, G.; Edwards, R.; Friedrich, M.; Grootes, P.; Guilderson, T.; Hajdas, I.; Heaton, T.; Hogg, A.; Hughen, K.; Kaiser, K.; Kromer, B.; McCormac, F.; Manning, S.; Reimer, R.; Richards, D.; Southon, J.; Talamo, S.; Turney, C.; van der Plicht, J., and Weyhenmeye, C., 2009. IntCal09 and Marine09 radiocarbon age calibration curves, 0–50,000 years cal BP. *Radiocarbon*, 51(4), 1111–1150.

Rowe, C., 2007. Vegetation change following mid-Holocene marine transgression of the Torres Strait shelf: A record from the island of Mua, northern Australia. *The Holocene,* 17(7), 927–937.

Saintilan, N. and Hashimoto, T., 1999. Mangrove-saltmarsh dynamics on a bay-head delta in the Hawkesbury River estuary, New South Wales, Australia. *Hydrobiologia,* 413(0), 95–102.

Satake, K. and Atwater, B., 2007. Long-term perspectives on giant earthquakes and tsunamis at subduction zones. *Annual Reviews of Earth and Planetary Sciences,* 35, 349–374.

Sawai, Y., 2001. Episodic emergence in the past 3000 years at the Akkeshi estuary, Hokkaido, northern Japan. *Quaternary Research,* 56(2), 231–241.

Sawai, Y.; Horton, B., and Nagumo, T., 2004. The development of a diatom-based elevation transfer function along the Pacific coast of eastern Hokkaido, northern Japan—An aid in paleoseismic studies of the Kuril subduction zone. *Quaternary Science Reviews,* 23(23), 2467–2484.

Sawai, Y. and Nasu, H., 2005. A 4500-year record of emergence events at Onnetoh, Hokkaido, northern Japan, reconstructed using plant macrofossils. *Marine Geology,* 217(1), 49–65.

Sawai, Y.; Satake, K.; Kamataki, T.; Nasu, H.; Shishikura, M.; Atwater, B.; Horton, B.; Kelsey, H.; Nagumo, T., and Yamaguchi, M., 2004. Transient uplift after a 17th-century earthquake along the Kuril subduction zone. *Science,* 306(5703), 1918–1920.

Schwartz, S.Y., 1999. Non-characteristic behavior and complex recurrence of large subduction zone earthquakes. *Journal of Geophysical Research,* 104(B10), 23111–23125.

Schwartz, S.Y. and DeShon, H., 2007. Distinct updip limits to geodetic locking and microseismicity at the northern Costa Rica seismogenic zone: Evidence for two mechanical transitions. *In:* Dixon, T. and Moore, J.C. (eds.), *The Seismogenic Zone of Subduction Thrust Faults*. New York: Columbia University Press, pp. 576–599.

Shennan, I.; Bruhn, R.; Barlow, N.; Good, K., and Hocking, E., 2014. Late Holocene great earthquakes in the eastern part of the Aleutian megathrust. *Quaternary Science Reviews,* 84, 86–97.

Sherrod, B.L., 1999. Gradient analysis of diatom assemblages in a Puget Sound salt marsh: Can such assemblages be used for quantitative paleoecological reconstructions? *Palaeogeography, Palaeoclimatology, Palaeoecology*, 149(1), 213–226.

Sieh, K.; Natawidjaja, D.; Meltzner, A.; Shen, C.; Cheng, H.; Li, K.; Suwargadi, B.; Galetzka, J.; Philisobian, B., and Edwards, R., 2008. Earthquake supercycles inferred from sea-level changes recorded in the corals of west Sumatra. *Science,* 322(5908), 1674–1678.

Sirkin, L., 1985. Late Quaternary stratigraphy and environments of the west Mexican coastal plain. *Palynology,* 9(1), 3–25.

Stein, S. and Okal, E., 2007. Ultralong period seismic study of the December 2004 Indian Ocean earthquake and implications for regional tectonics and subduction processes. *Bulletin of the Seismological Society of America,* 97(1A), S279–S295.

Wang, P. and Horwitz, M., 2007. Erosional and depositional characteristics of regional overwash deposits caused by multiple hurricanes. *Sedimentology,* 54(3), 545–564.

Yue, H.; Lay, T.; Schwartz, S.; Rivera, L.; Protti, M.; Dixon, T.; Owen, S., and Newman, A., 2013. The 5 September 2012 Nicoya, Costa Rica M_w 7.6 earthquake rupture process from joint inversion of high-rate GPS, strong-motion, and teleseismic P wave data and its relationship to adjacent plate boundary interface properties. *Journal of Geophysical Research: Solid Earth,* 118(10), 5453–5466.